UDC 691 . 714 : 539 . 413

Strength of Structural Elements for Steel-Framed Houses

Koji HANYA*1 Ryoichi KANNO*1
Nobuyoshi UNO*1

Abstract

Steel-framed houses are made up of panels, which are composed of steel channels and sheathings such as gypsum boards and plywood with self-drilling screws. In design, the panels are generally designed such that only the channels can resist external forces, and the composite actions of the panels are scarcely considered. It is, however, observed in some cases that the panels show larger strength than those calculated based on the strength only of the channels. In this paper, especially for the panels composed of plywood and steel channels, the composite actions of both materials and the buckling restraint effect of the channels were studied based on experiments and analyses. New design methods taking into account the composite actions were proposed that make the steel houses more economical and improve the strength.

1. Introduction

Steel-framed houses are based on the wood-frame construction used widely in the US[1]. They are built with 0.8 to 1.6 mm thick galvanized light-gauge steel channel shapes (hereinafter referred to as channels)[2] and sheathing such as 9 to 15 mm thick structural plywood and gypsum board. Basic structural components are panels assembled by fastening sheathing to channels with self-drilling screws[3]. These panels are interconnected to form the floors, walls, and roofs of steel-framed houses (see **Fig. 1**).

In steel-framed houses, the structural elements are rarely designed as panels in which the sheathing is fastened integrally with the channels, except for the design of bearing walls and floors against in-plane shear forces[4]. The elements are generally designed as channels singly resisting external forces[5]. Through some experiments[6-8], however, the authors have noticed cases in which the flexural strength of panels reaches several times higher than the calculated strength of channels alone and have confirmed that the combined effect of the sheathing and channels is not small. It is thus important that in addition to the member characteristics of channels, the structural characteristics of channels as panels should be investigated and adequately reflected into the design of steel-framed houses.

From this background, this study is designed to investigate experimentally and analytically the effect of the combination of the channels and sheathing in increasing the flexural strength of the re-

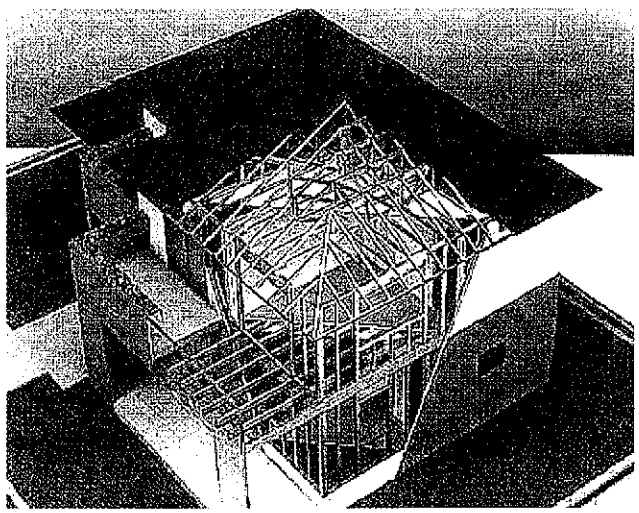

Fig. 1 Structure of steel-framed house

*1 Technical Development Bureau

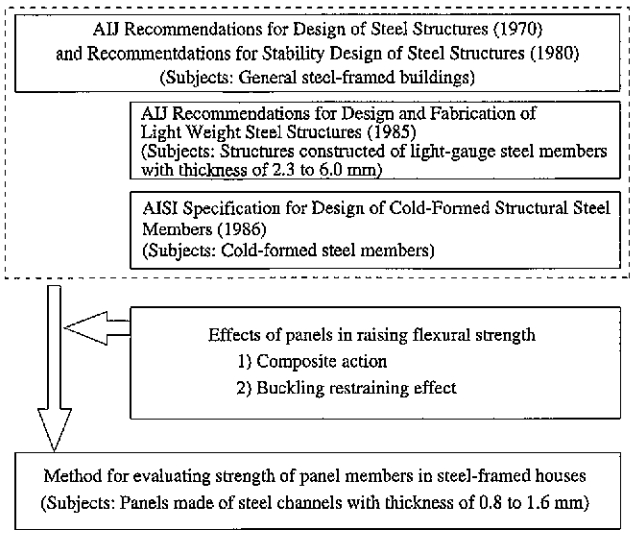

Fig. 2 Relations of this report with existing design methods

sultant panel and to propose new design methods for steel-framed houses (see **Fig. 2**). Here, the effect of the combination of the channels and sheathing in increasing the flexural strength of the panel is handled in two separate parts: 1) the composite action whereby the sheathing shares and resists the external forces together with the channels ; and 2) the buckling restraint effect whereby the sheathing restrains the buckling of the channels. Steel members with a thickness of about 1 mm, the subject in this study, have been actively investigated in Europe and the United States[9,10], and the design guidelines have been established for them[11]. To the authors' knowledge, however, there are no papers published concerning the effects of the sheathing in increasing the flexural strength of the panels composed or structural plywood and channels.

2. Panels in Steel-Framed Houses

The panels that comprise a steel-framed house can be divided into three groups: wall, floor, and roof panels. When an attention is focused on their cross-sectional composition, the panels may be divided into two types: one type sheathed on both sides and the other type sheathed only on one side (see **Fig. 3**). For wall panels, vertical forces due to the dead load and the like and horizontal forces due to the seismic and wind loads become main external forces. The wall panels act as an element that resists the in-plane compressive force and shear force produced. For floor and roof panels, on the other hand, vertical forces due to the dead load, snow load and the like become main external forces. They act as an element that resists the out-of-plane bending moment.

The effect of sheathing in the present design of steel-framed houses[5] is handled differently with the type of panel and the force applied. For example, the sheathing is assumed to carry the shear force produced in plane, but its out-of-plane bending is ignored. Concerning the buckling restraint effect, a wall sheathed on both sides is considered to have the flexural buckling of the channels in the direction of the weak axis (wall in-plane direction) restrained by the sheathing. When the roof and floor panels sheathed only on one side are subjected to such a bending moment that the flange in contact with the sheathing is in compression, the lateral buckling of the channel is thought to be fully restrained. When the sheathing is in tension, conversely, the effect of the sheathing in restraining the buckling of the channel is considered to be unclear and is ignored.

Of these panels, the roof and floor panels are studied in this paper. The roof and floor panels have plywood applied to one side of the channels as shown in **Fig. 4** and are mainly subjected to the out-of-plane bending moment produced by the dead load and live load, among other things (see **Fig. 5**, for example). The bending moments that act on these panels can be divided into two types, positive bending moment and negative bending moment, as shown in **Fig. 6**. The positive bending moment produces a compressive force in the flange of the channel to which plywood is fastened, while the negative bending moment produces a compressive force in the flange of the channel to which plywood is not fastened. These two stress conditions greatly differ in the composite action and the buckling restraint effect, so that they are treated with clear distinction in the chapters that follow.

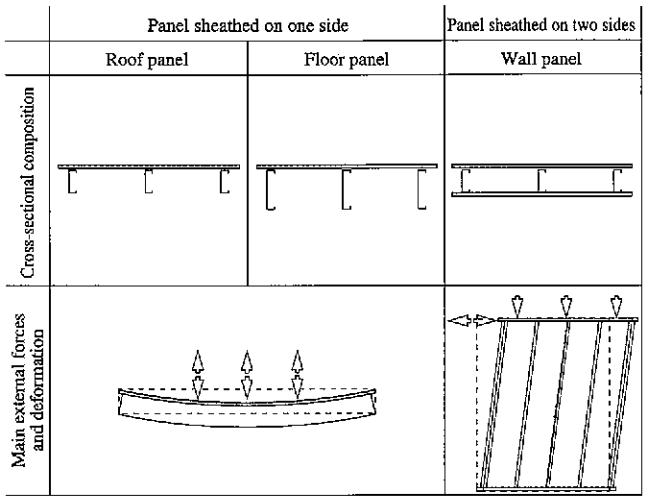

Fig. 3 Classification of panels

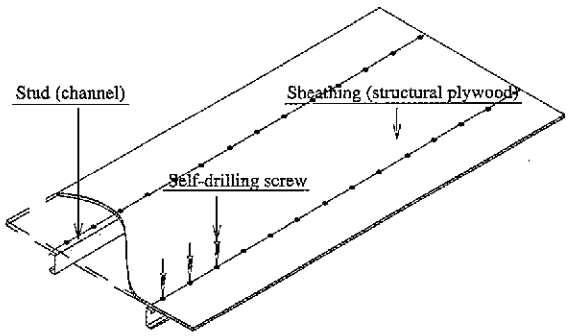

Fig. 4 Panel studied

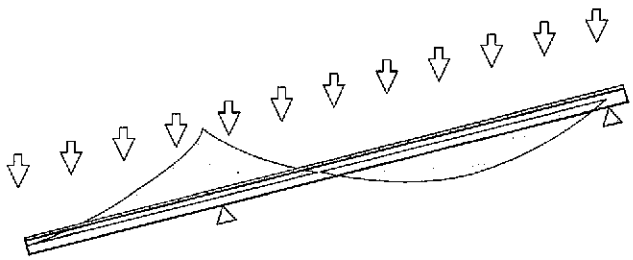

Fig. 5 Representative moment distribution in roof

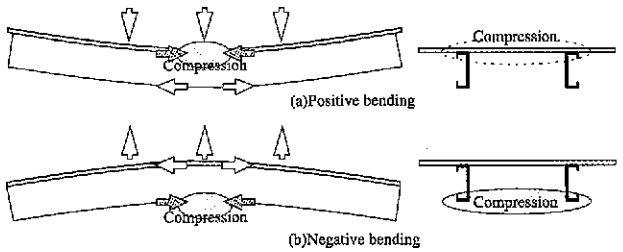

Fig. 6 Positive and negative bending of panels

3. Panel Bending Tests and Load Carrying Capacities

This chapter outlines the out-of-plane bending tests conducted to study the bending properties of panels, and discusses the load carrying capacity, composite action, buckling restraint effect and other details of panels.

3.1 Outline of panel bending tests[6,7]

Each specimen was a panel made by connecting structural plywood (JAS Class 1, 9 mm thick) to channels with self-drilling screws (4.2 mm in diameter), and was tested under four-point bending as shown in **Fig. 7**. Since the load carrying capacity of the panel differs with the direction of the bending action, two types of bending tests, a positive bending test as shown in Fig. 7(a) and a negative bending test as shown in Fig. 7(b), were carried out. In the negative bending test, a short timber whose both ends are cut like a knife edge was placed below each loading point so that the distance between the loading points (L_b) was made as equal as possible to the unbraced length of the channels. The timber also serves to uniformly distribute the load throughout the panel.

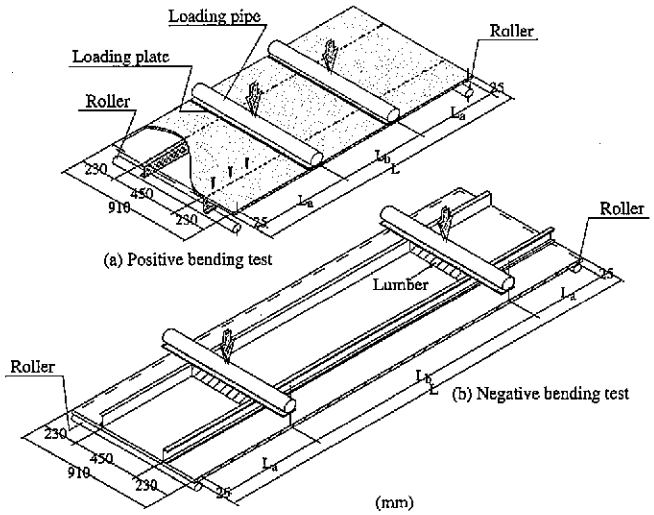

Fig. 7 Test specimens and loading methods

The test parameters were: 1) the direction of action of the bending moment (positive or negative as shown in Fig. 7); 2) spacing of self-drilling screws; 3) distance between the loading points L_b; and 4) geometry of channels (with or without lips as shown in **Table 1**).

The positive bending test series included non-lipped channels to obtain additional data, although lipped channels are normally used in the roofs and floors of steel-framed houses. The spacing of self-drilling screws was varied within the range of 25 to 200 mm to investigate the composite action of the panel sheathing and studs. For the negative bending test series, only lipped channels were used and the spacing of self-drilling screws was not changed. Instead, L_b was changed as the parameter to investigate the effect of the unbraced length.

3.2 Behavior under positive bending and composite action[6]

Fig. 8 and Table 1 show the test results in comparison with the values of strength calculated by the evaluation method[5] employed usually in Japan for the design of steel-framed houses. The calculated strength is the flexural strength of channels alone. It is based on the local buckling strength[5] of the channels because it is assumed in this case that the lateral buckling of the channels is restrained by the sheathing. In the strength calculation, the measured yield strength σ_y of the channel is used. From Fig. 8, it can be seen that the initial stiffness and maximum strength both increase as the self-drilling screw spacing decreases from 200 mm. When the screw spacing is the minimum 25 mm, the initial stiffness and maximum strength are both higher by about 40% for the lipped channels and by about 80% for the non-lipped channels than when the spacing is the maximum 200 mm. The observed values of strength are all higher than the calculated values of strength. As the number of self-drilling screws used is increased in this way, the channels and plywood increase in their unity and deliver a greater composite action.

The specimens behave similarly, irrespective of whether or not the channels are lipped. The maximum strength is governed by the local buckling of the channel flange and web in compression (see **Photo 1**). The failure of the screw connections proceeds at the same

No.	Symbol	Thickness (mm)	Yield point σ_y (MPa)	Tensile strength σ_u (MPa)	Shape and dimensions (mm)	Test method	Total length (mm)	Pure bendign span L_b (mm)	Shear span L_a (mm)	Screw spacing (mm)	Test results: Maximum strength (kN·mm²)	Test results: Initial stiffness (kN·mm²)	Calculated strength of channels alone (kN·mm)
1	NL-25	0.81	289	392	90, 25	Positive bending	1,820	590	590	25	3,010	96.9	1,479
2	NL-50									50	2,884	75.6	
3	NL-100									100	2,123	65.6	
4	NL-200									200	1,619	55.8	
5	L-25	0.79	308	405	90, 25, 10	Positive bending	1,820	590	590	25	3,382	94.3	1,952
6	L-50									50	3,133	79.4	
7	L-100									100	2,574	74.0	
8	L-200									200	2,340	66.2	
9	LR-500	0.79	308	405	90, 25, 10	Negative bending	1,820	500	635	100	1,736	-	1,668
10	LR-910						1,820	910	430		1,874	-	674
11	LR-1,200						1,820	1,200	285		1,696	-	388
12	LR-1,600						2,730	1,600	540		1,780	-	218

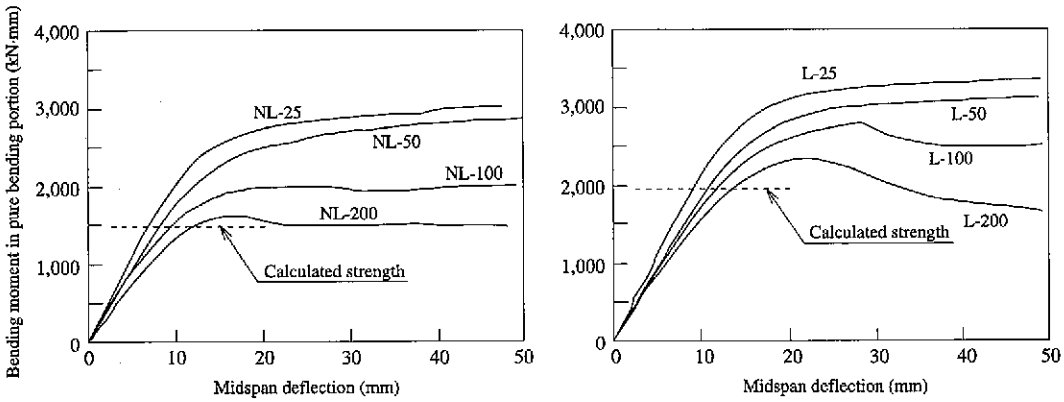

(a) Non-lipped channels (b) Lipped channels

Fig. 8 Positive bending test results of panels

time as the buckling of the channel. The inclination of the screws is observed in the shear span portion (see **Photo 2**). The lipped channels are higher in maximum strength than the non-lipped channels. This is due to the difference in the local buckling strength between the lipped and non-lipped channels.

Fig. 9 shows the strain distribution in the cross section of each channel at the midspan. For ease of comparison, each distribution is shown when the strain (ε_{up}) in the channel flanges is about 750×10^{-6}. In Fig. 9, M_m is the bending moment in the pure bending portion where each strain distribution is produced, and ε_w at the topmost position is the strain developed in the plywood. From the strain distribution, it is known that Navier's hypothesis practically holds when the spacing of the self-drilling screws is 25 mm. It is also seen that as the spacing of the self-drilling screws increases, the difference between the flange strain ε_{up} and the plywood strain ε_w increases, meaning that Navier's hypothesis no longer holds. Fig. 9 shows that increasing the spacing of the self-drilling screws pushes down the neutral axis of the channel section, with the result that the strain in the upper compression flange to which the plywood is fastened is more likely to increase. The measured strain values indicate the tendency for the channel flanges to locally buckle around when their strain reaches the yield strain ε_y.

As discussed above, the composite action of the panel is large in the positive bending condition. It is necessary to establish rational design methods that take this effect into account.

3.3 Behavior under negative bending and buckling restraint effect[7]

Fig. 10 shows the negative bending test results of the panels. Since the specimens are different in span and other conditions, it should be noted that direct comparison of their load-displacement curves is meaningless. The calculated values of strength are shown in Table 1 and Fig. 10. The calculated strength is lateral buckling strength of the channels alone[5,12]. In the calculation, the unbraced length is assumed to be the distance between the two loading points L_b, and the measured yield strength through material testing is used.

The specimens behave similarly each other during negative bending. They exhibit elastic behavior before they reach the maximum strength caused by the buckling of the channels. LR-1200 exhibits results somewhat different from those of the other specimens because it simultaneously had local deformation near the supports. The negative flexural strengths are found to be about 50 to 70% of the positive flexural strengths shown in Fig. 8(b). The buckling mode of

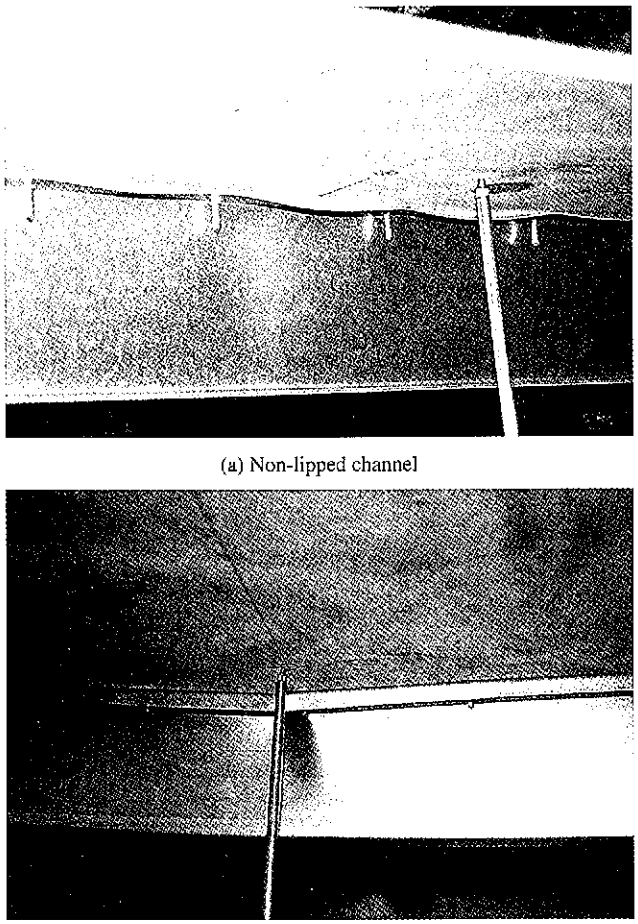

(a) Non-lipped channel

(b) Lipped cahannel

Photo 1 Local buckling of compression flange in positive bending test

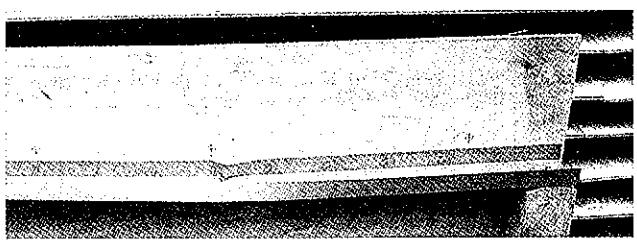

Photo 2 Inclination of self-drilling screws in shear span

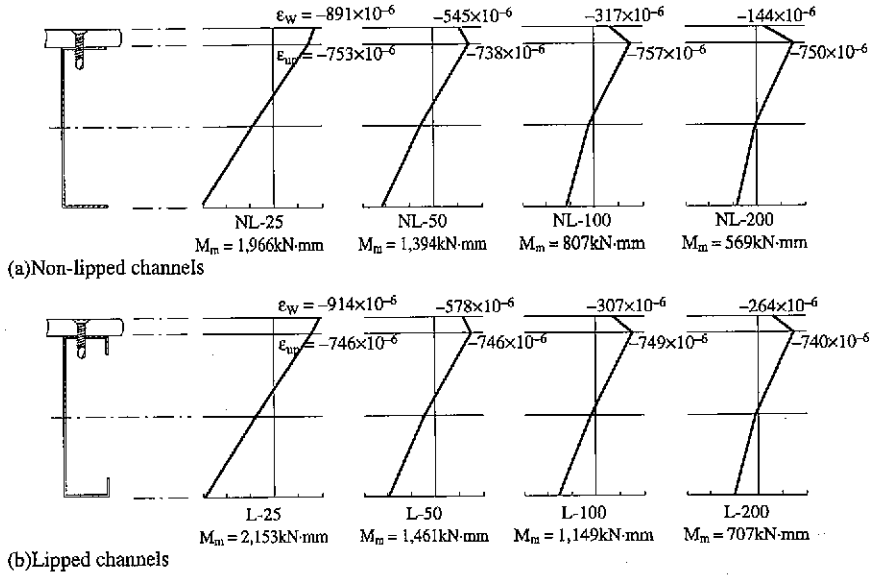

Fig. 9 Strain distribution (observed values when $\varepsilon_{up} = 750\times10^{-6}$)

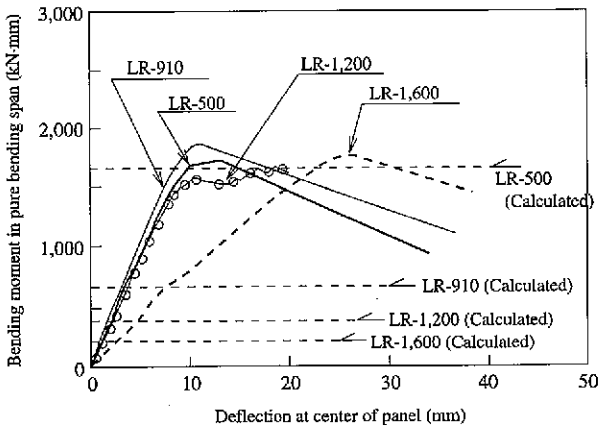

Fig. 10 Negative bending test results of panels

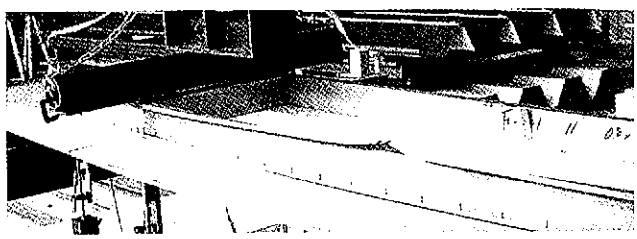

Photo 3 Buckling of channels in negative bending test

the negative bending specimens was different from lateral buckling, which is the typical buckling mode of panels without sheathing. The flanges and web were partially moved laterally, and the channels were deformed in cross section (see **Photo 3**). The observed values of strength are markedly different from the calculated of strength. For the lateral buckling that a panel undergoes when it is constructed of channels alone, the buckling strength decreases with increasing unbraced length. In the negative bending tests, the specimens have little drop in strength with increasing unbraced length. The observed strength of LR-1600 with the longest unbraced length is about 8 times higher than its calculated strength.

As discussed above, the calculated strength that does not consider the presence of sheathing differs greatly from the actual strength in the negative bending condition. Ignoring the sheathing results in an uneconomical design. It thus becomes an important issue to establish design methods that allow for the effect of sheathing. Experimental results suggest that the composite action observed in the positive bending test is relatively small under the action of negative bending. This composite action may be ignored without any design problems for the negative bending.

4. Positive Flexural Strength with Composite Action

Based on the experimental results discussed in Chapter 3, a method is proposed here for evaluating the strength of panels subjected to positive bending by considering the composite action of the channels and plywood. By referring to the method for evaluating the strength of composite beams of steel and concrete[13], the panel strength evaluation method is first studied for fully composite panels of channels and plywood and then expands its application to partially composite panels.

4.1 Strength evaluation for fully composite panels

When the channels and plywood are assembled into a fully composite panel, Navier's hypothesis can be assumed to hold for the cross section of the panel. Fig. 11(a) shows the distribution of strains in the cross section of a fully composite panel when subjected to positive bending. The strain in the compression flange of the channel is defined ε_{up}, and the strain in the plywood is ε_w. For simplification, the strain in the plywood is assumed to be constant through the thickness, and when the panel is fully composite, ε_{up} and ε_w are assumed to be equal in value. The plywood thickness is t_p, and Young's modulli of the channels and plywood are E_s and E_p (= 7,680 MPa), respectively.

To calculate the maximum strength of panels, it is necessary to define a condition when the panel reaches its maximum strength. According to the test results discussed in Chapter 3, the maximum strength is dominated by local buckling and shown to the strength when the compression flange approximately reaches the yield strain

ε_y of the material. In this paper, therefore, the channel is assumed to be at the maximum strength when the compression flange reaches ε_y. This consideration is also seen for calculating the ultimate flexural strength of channels in the Specification for the Design of Cold-Formed Steel Structural Members of the American Institute of Iron and Steel (AISI)[11].

Introduction of this condition produces a strain distribution for a fully composite panel as shown in **Fig. 11**(a). A corresponding stress distribution is defined as shown in Fig. 11(c). The distance x_a that indicates the position of the neutral axis can be calculated from the condition that the sum of the resultants P_{wc}, C_1, C_2, T_1, T_2, and T_3 shown in Fig. 11(c) should become zero. The calculation of C_1, C_2, T_1, T_2, and T_3 considers the effective width corresponding to the yield strength σ_y, determined based on those like the steel structure design standard[19]. Calculation of P_{wc} calls for the effective width b_e of the plywood due to shear lag. From the observed strain distribution in the plywood, the effective width b_e is set here on the safe side as a half of the plywood width supported with each channel. In the stress distribution of Fig. 11(c), it should be noted that since at maximum strength the strain in the compression flange is imposed to ε_y, the entire tension flange region and part of the web in tension (region x_p) are yielded.

If the moment M about the neutral axis is calculated from the stress distribution of Fig. 11(c), the positive flexural strength of the fully composite panel can be obtained. The calculated and observed values of the positive flexural strength for the fully composite panels are comparatively shown by the bars at the left end of **Figs. 12**(a) and 12(b). The horizontal arrows indicate the experimental results. The calculated strengths of the fully composite panels are almost the same as the observed strengths of NL-25 and L-25 with the closest self-drilling screw spacing. This suggests that the proposed evaluation method provides reasonable strength estimates.

4.2 Strength evaluation for partially composite panels

It is not easy from a construction point of view to connect the channels and plywood with as many self-drilling screws as required to produce a fully composite panel. For this reason, the authors propose here a method for evaluating the strength of partially composite panels.

As observed in the tests of Chapter 3, as the self-drilling screw spacing increases and the unity of the channels and plywood decreases, the difference between the channel compression flange strain and the plywood strain increases, and the panel fails to satisfy Navier's hypothesis. This strain difference moves down the neutral axis to the tension side and causes the channel compression flange to reach the yield strain ε_y under a smaller load. As a result, the panel locally buckles at a small load level and reaches the maximum strength.

Here, attention is focused on the strain difference. The ratio of the plywood strain ε_w to the channel compression flange strain ε_{up} is defined as the composite ratio k_c and used to evaluate the strength of partially composite panels. When the composite ratio k_c is introduced, the plywood strain is obtained as $\varepsilon_w = k_c \cdot \varepsilon_{up}$ as shown in Fig. 11(b). If the strength at which ε_{up} reaches ε_y is taken as the maximum strength, the panel strength can be calculated in the same way as described for fully composite panels in the preceding section.

Fig. 12 shows the calculated flexural strength of the panels when the composite ratio k_c is changed in the entire range of 0 to 100%. The contributions of the channels and the plywood to the flexural strength of the panel are also shown in Fig. 12. As the composite ratio increases, the contribution of the plywood increases at higher rates, and as a result the whole flexural strength of the panel increases. From a comparison of the calculated and observed values, the composite ratio of each specimen can be estimated.

To calculate the strength of a partially composite panel by this method, it is essential to set the composite ratio k_c for the panel de-

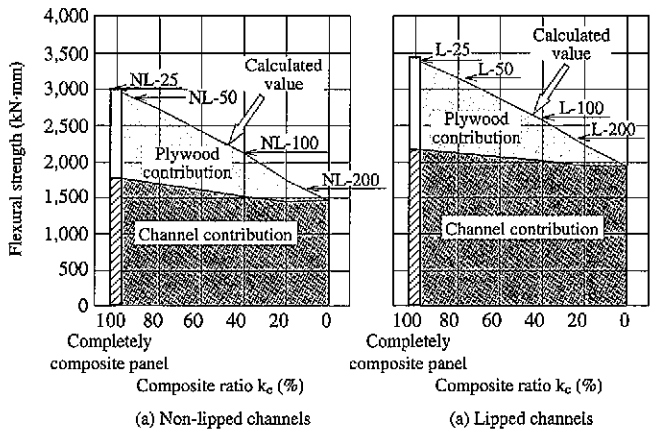

Fig. 12 Composite ratio k_c and flexural strength

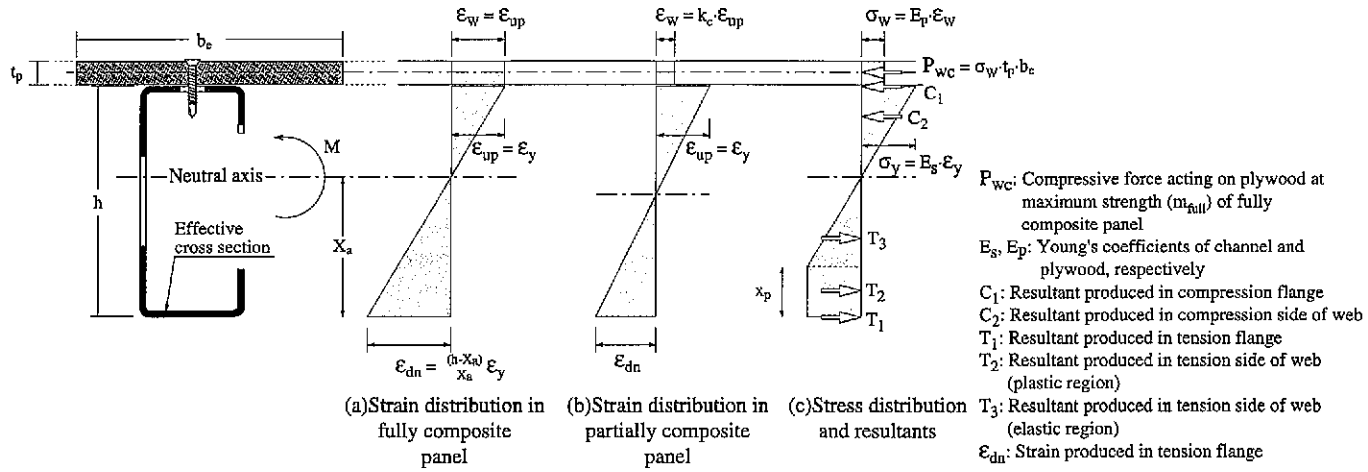

Fig. 11 Strain and stress distributions in positive flexural strength evaluation

signed. Here, study was carried out based on consideration for steel-concrete composite beam strength evaluation[13]. **Fig. 13** shows the test conditions described in Chapter 3. The composite action of a panel depends on the shear force transmission capability between the channel and the plywood in the shear span L_p governed by the point at which the moment is zero and the point at which the moment is maximum. Let $n \cdot P_v$ be the total shear strength of the self-drilling screws driven in the L_p (P_v = maximum shear strength per self-drilling screw and n = number of self-drilling screws driven in the L_p), and P_{wc} be the compressive force acting on the plywood when the fully composite panel reaches the maximum strength M_{full} [P_{wc} can be calculated by the method shown in Fig. 11(c)]. Here, P_{wc} is the force that must be transmitted by the self-drilling screws to make the panel fully composite, and $n \cdot P_v$ is the resistance. The $n \cdot P_v / P_{wc}$ ratio can be thus used as a measure of the composite action of the panel.

Based on comparison with the experimental results, it was known that the relationship between the ratio $n \cdot P_v / P_{wc}$ and the composite ratio k_c is assumed as shown in **Fig. 14**. The values of strength calculated based on Fig. 14 are shown in comparison with the observed values of strength in **Fig. 15**. Here, P_v was set as P_v = 1,400 N according to the results of shear tests separately conducted on self-drilling screw connections between plywood and steel plate. From Fig. 15, it can be seen that the calculated values provide good strength estimation.

Similarly for a more general simple beam case with an overhang (see **Fig. 16**), $n \cdot P_v / P_{wc}$ may be obtained for each distance L_p in the positive bending region where the composite action is expected, and k_c for each L_p is then determined from the $n \cdot P_v / P_{wc}$. The model proposed in this chapter allows yielding to occur in the tension side at the maximum strength and calls for care, for example, when determining the safety factor.

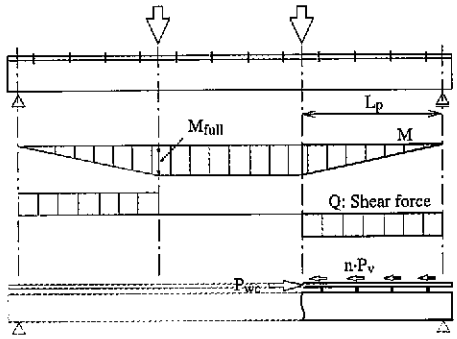

Fig. 13 Relationship between P_{wc} and $n \cdot P_v$ in equal bending test

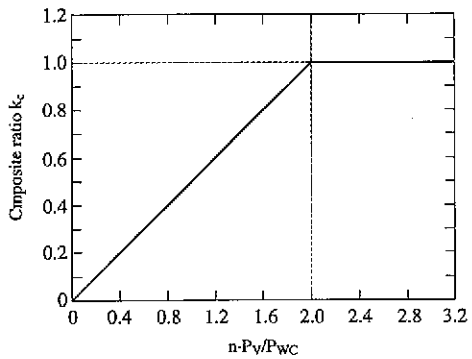

Fig. 14 Relationship between composite ratio k_c and $n \cdot P_v / P_{wc}$

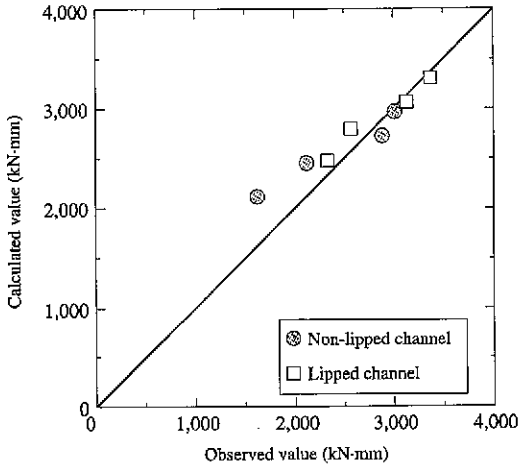

Fig. 15 Comparison of observed and calculated values of flexural strength

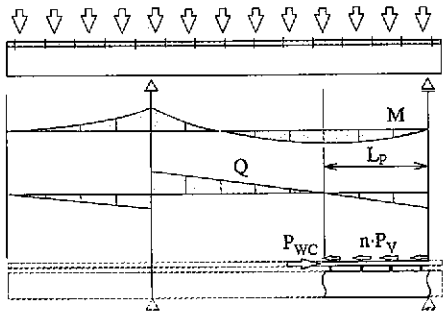

Fig. 16 Consideration under general conditions

4.3 Trial study in steel-framed houses

Attempt was made to calculate the strength of typical roof and floor by considering the composite action. The panels are a roof panel composed of steel channels 89LCN12 (C89×40×12×1.2) and 9 mm thick plywood, and a floor panel composed of steel channels 235LCN12 (C235×40×12×1.2) and 15 mm thick plywood. The calculation of strength assumed each panel as a simple beam subjected to a uniformly distributed load, and assumed a span of 1.82 m for the roof panel and a span of 2.73 m for the floor panel. The channels were assumed to be arranged 455 mm apart, and the strength was calculated per channel.

The strength of the panels was calculated in three cases (see **Fig. 17**). In one case, self-drilling screws with a diameter of 4.2 mm were driven at a spacing of 300 mm (300), a standard spacing for steel-framed houses. In another case, the composite ratio was assumed to be zero. In the last case, the panel was assumed to be fully composite. The strengths of both 89LCN12 and 235LCN12 in the case of 300 are increased by about 10% as compared with the cases of the zero composite ratio. The strengths of the panels in the case of 300 are about 70 and 90% of those for the fully composite 89LCN12 and 235LCN12, respectively. Through these calculations, it is known that a strength increase of about 10% can be expected in the standard case of 300. It is also noticed that a further strength increase is possible for the channels with lower web depth. To deliver the composite action, it becomes necessary to improve the connection between the channel and the plywood. Since increasing the number of self-drilling screws increases the difficulty of construction, improvement in strength per self-drilling screw and/or use of adhesive will have to

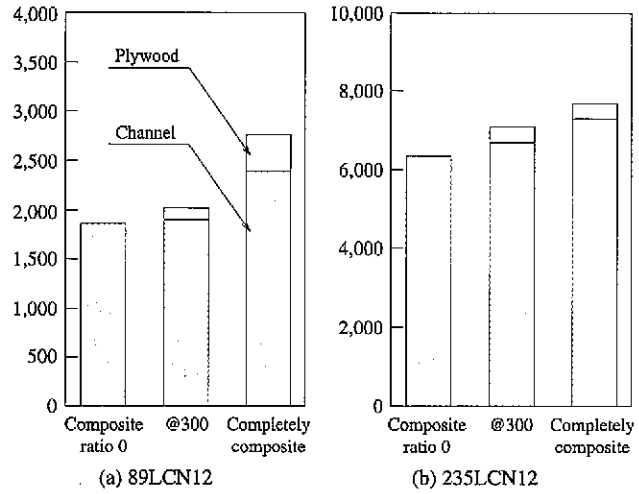

Fig. 17 Concrete study of steel-framed house members

be studied in the future.

Use of channels with larger web depth (for example, 235LCN12) must be investigated further, because the validity of the proposed evaluation method is not yet verified and because if the composite action is increased further, the strain and yield region of the steel in tension are feared to increase at the time of ultimate strength.

5. Negative Flexural Strength with Buckling Restraint Effect

This chapter discusses the buckling restraint effect of panels subjected to negative bending on the basis of elastic buckling analysis, and proposes a method for evaluating the strength of panels. The composite action of the sheathing and the channels during negative bending described in Chapter 3 is so small that it is not considered here.

5.1 Elastic buckling analysis and distortional buckling

To investigate the buckling characteristics of panels in greater detail, elastic buckling analysis was performed on the negative bending test specimens described in Chapter 3. The analysis used the elastic analysis program THIN-WALL[14,15] based on the finite strip element method (FSM) and developed at the University of Sydney. The program uses strip elements that approximate the buckling mode of a member in the axial direction by half-waves of a sine function and in the transverse direction by polynomial functions. The cross section of the member is divided into strip elements. This analysis assumes that the member has uniform cross-sectional shape in the axial direction, as well as uniform thickness and applied stress.

The analytical mode of a panel in the negative bending condition is shown in **Fig. 18**. Since the composite action is ignored here, the stress distribution is assumed such that the neutral axis N is located at the center of the web. The self-drilling screw connection with plywood is modeled by restraining the displacement in the x and y directions and the rotation about the z axis. The analysis was carried out by changing the member length (denoted by L_h and called the halfwave length here), and the changes in the buckling mode were investigated.

In addition to the analysis shown in Fig.18, the analysis of panels without the plywood restraint and the analysis of panels in the positive bending were also performed for comparisons. The neutral axis actually moves due to the composite action during positive bending but it was ignored. The results of the three cases are shown in **Fig. 19**, where the elastic buckling strength σ_{cr} expressed in the stress of the channel outermost fiber is plotted along the vertical axis and the halfwave length is plotted along the horizontal axis. The typical buckling modes that appear in each case are also shown in Fig. 19. As the halfwave length increases, the negative bending panel changes its buckling mode from local buckling (mode 1-2) to buckling (mode 2-2) with the lateral movement of flanges and then to buckling (mode 4) with the lateral movement of web. The buckling modes 2-2 and 4 involving the cross-sectional deformation are similar to the modes observed in the negative bending tests. This suggests that the buck-

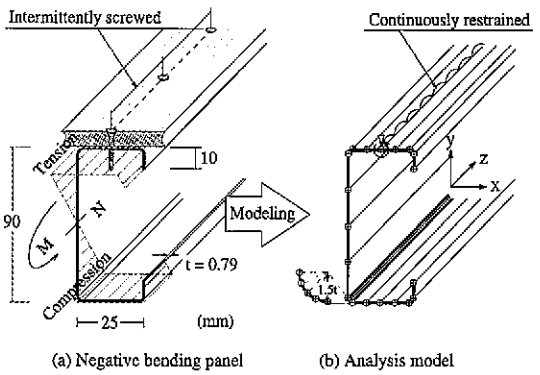

Fig. 18 Modeling of panel for buckling analysis

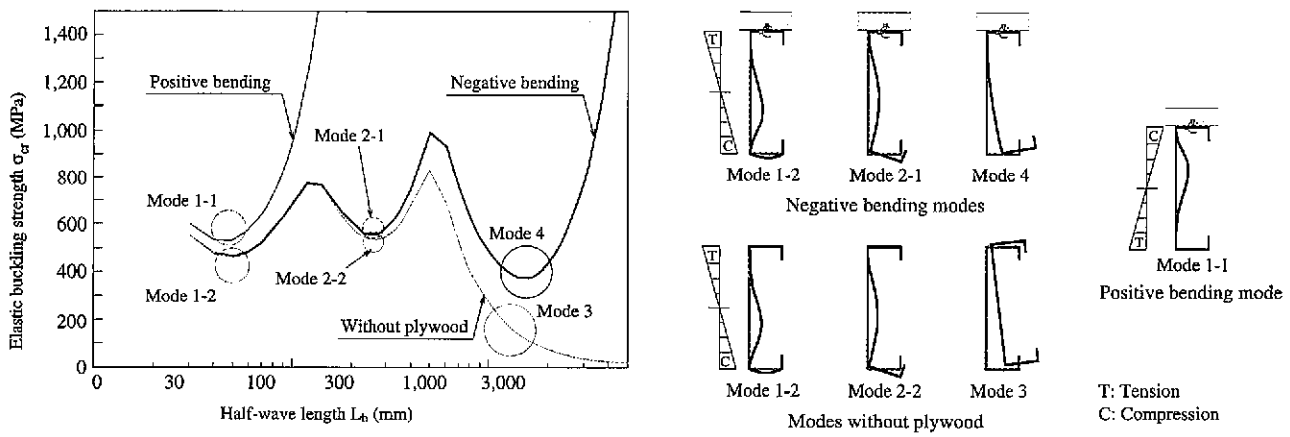

Fig. 19 Elastic buckling strength and buckling modes

ling analysis can evaluate actual buckling modes well.

For the analysis of the channels alone (without the plywood), modes 1 and 2 are similar to those observed in the negative bending tests. As the halfwave length increases further, the shift to lateral buckling in mode 3 is appeared.

From these results, it can be understood that the plywood fastened to the tension flange of the channel has the effects of preventing the occurrence of lateral buckling (mode 3), causing another buckling mode (mode 4) involving cross-sectional deformation, which delivers a greater buckling strength. When the panel is composed of channels alone, its buckling strength monotonically decreases with increasing the halfwave length. When the panel is composed with the plywood, however, its buckling strength has a minimum value due to the buckling restraint effect by the plywood. Buckling involving a cross-sectional deformation, represented by mode 4, is called distortional buckling and handled differently from local buckling and global buckling. It has been a subject of active research in recent years.

The case of panels subjected to positive bending as shown in Fig. 19 is different from the other two cases. Since the portion subjected to compression is directly restrained by the plywood in this case, distortional buckling and lateral buckling do not occur, but local buckling alone occurs. This result also agrees with the experimental observation discussed in Chapter 3.

As noted above, in the case of panels subjected to negative bending, lateral buckling is restrained by the plywood, and distortional buckling occurs as another mode and raises the buckling strength of the panel. In current steel structure design guidelines[5,12,18] in Japan, this distortional buckling is not considered. Therefore, strength evaluation methods that can properly evaluate the distortional buckling are required.

5.2 Strength evaluation in consideration of distortional buckling

For evaluating of the negative flexural strength of panels, elastic buckling strength becomes a basis. The distortional buckling results alone are extracted from the results in Fig.19 and are shown in **Fig.20**. Note that this set of data cannot be directly used to evaluate the buckling strength of the panels. The finite strip element method applied in this paper cannot evaluate complicated modes like simultaneously occurring buckling modes, because the buckling mode in the direction of action of stress on the strip elements is approximated by half waves of a sine function. To obtain actual elastic buckling strength curves from the analysis results, it is necessary to consider the fact that a buckling mode and strength that occur at a given halfwave length are governed by the point at which the strength becomes minimum below the given halfwave length. As a result, the envelope curve indicated by the dotted line in Fig. 20 shows the actual elastic buckling strength used for buckling strength evaluation. According to the dotted line in Fig. 20, regions A and B are governed by modes 2 and 4, respectively.

In the evaluation of buckling strength, it is necessary to consider the effects of material yielding, geometric imperfections and residual stresses, and coupling with local buckling. For the case of column buckling[9], the effect of material yielding is taken into account by applying Johnson's parabolic formula[19]. As for the coupling with local buckling, the effect is considered through multiplying the buckling strength σ_{cr} by the cross-sectional area obtained based on the effective width. It is assumed in this paper that for distortional buckling, those effects are considered by a similar manner to that for the columns buckling. Similar evaluation methods for distortional buckling have already been presented by Kwon and Hancock[17] and Serrette and Pekoz[18] for steel channel columns and steel sheet roofs.

The strength evaluation method for distortional buckling proposed in this paper is summarized in **Fig. 21**. The lateral buckling strength evaluation method[5,12] currently used for the design of steel framed house is also shown for reference. Both current and proposed methods shown in Fig.21 are relatively comparable. The method of calculating the elastic distortional buckling strength in step 1 can be based on the finite strip element method (FSM) previously described in this paper (as indicated by the dotted line in Fig. 20). In the calcu-

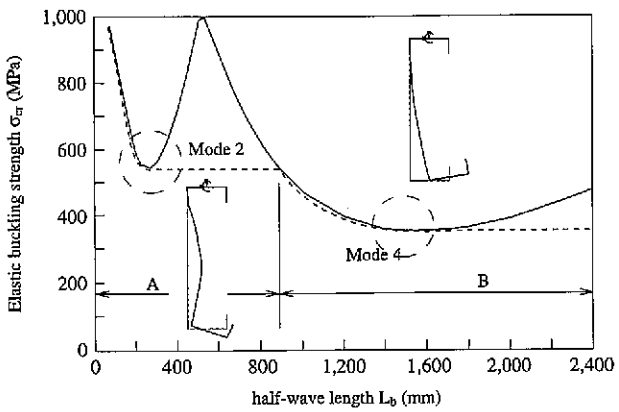

Fig. 20 Distortional buckling strength and modes

Buckling strength evaluation method (for channels)	Proposed distortional buckling strength evaluation method
Step 1: Calculation of elastic buckling strength	
Elastic lateral buckling strength $\sigma_{cre} = \frac{1}{2}\frac{C_1\pi^2 E}{(L_b/i)^2}$ C_1: Coefficient indicating effect of moment distribution i: Radius of gyration of area, E: Young's modulus	Elastic distortional buckling strength $\sigma_{crd} = \left\{\begin{array}{l}\text{Calculation based on buckling model}\\ \text{Calculation based on FEM}\\ \text{Calculation based on FSM, etc.}\end{array}\right\}$
Step 2: Calculation of buckling strength σ_{cr} based on Johnson's formula	
When $\sigma_{cre} > 0.6\,\sigma_y$, $\sigma_{cr} = \sigma_y\left(1.1 - 0.3\frac{\sigma_y}{\sigma_{cre}}\right) \leqq \sigma_y$ When $\sigma_{cre} \leqq 0.6\sigma_y$, $\sigma_{cr} = \sigma_{cre}$	When $\sigma_{crd} > 0.5\sigma_y$, $\sigma_{cr} = \sigma_y\left(1 - 0.25\frac{\sigma_y}{\sigma_{crd}}\right) \leqq \sigma_y$ When $\sigma_{crd} \leqq 0.5\sigma_y$, $\sigma_{cr} = \sigma_{crd}$
Step 3: Calculation of flexural strength M_{cr} by considering coupling with local buckling	
Flexural strength $M_{cr} = Z_e\sigma_{cr}$ where Z_e = section modulus calculated from effective width	

Fig. 21 Proposed buckling strength evaluation method in comparison with that used for channels in Japan

lation of buckling strength by the Johnson formula in step 2, the coefficients in the left and right sides of the equations are slightly different due to the differences in the evaluation of strain hardening and the material proportional limit. In step 2, σ_y is the yield strength of the material, but for the design stage, it should be replaced by the material design strength defined as F value in Japan. In step 3, Z_e is the effective section modulus calculated based on the effective width given in Japan[19,5], which corresponds to the F value (σ_y is used instead for comparison with the experimental results).

Following the proposed method in Fig.21, the calculated strengths and test results are compared in **Fig.22.** Note in Fig.22 that it is assumed that the halfwave lengths defined in the finite strip analysis are equal to the unbraced lengths of the test specimens. Fig. 22 includes the results of another series of experiments not reported here (indicated by the shaded circles), and the strength calculated by the method ignoring the buckling restraint effect of plywood. From Fig. 22, the proposed method provide good strength estimates to the test results. Through the comparison between the proposed and current methods, it is known that the proposed method can provide an economical design especially in the longer unbraced length region.

When evaluating the distortional buckling strength of panels in actual design, it is difficult to give an accurate halfwave length. For this reason, it is considered necessary to evaluate the smaller of the strengths in modes 2 and 4 shown in Fig. 20 as the distortional buckling strength.

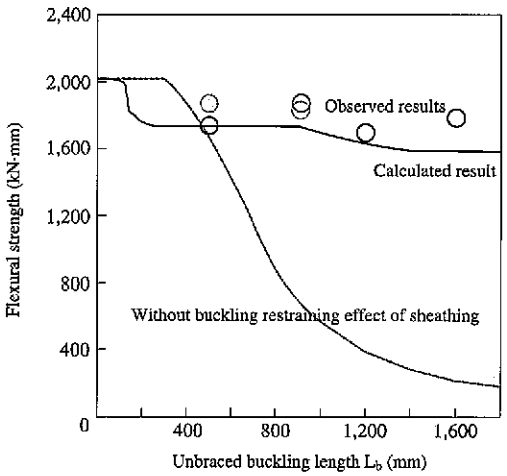

Fig. 22 Comparison of observed and calculated values of flexural strength

5.3 Trial study in steel-framed houses[20]

Steel channels for the floor joists, rafters, and other structural members of a steel-framed house were studied by the proposed method described in the preceding section. Three types of channels were studied: 235LCN12 (C235×40×20, t = 1.2), 140LCN12 (C140 ×40×12, t = 1.2), and 89LCN12 (C89×40×12, t = 1.2). The relationship between the short-term allowable flexural strength σ_{cr} and the unbraced length L_b of each type of channel calculated by using a F value of 280 MPa are shown in **Fig. 23**. For a comparison, the values of σ_{cr} calculated without considering the buckling restraint effect of the sheathing are also shown. As the channel increases in web depth, its σ_{cr} value decreases but remains in the range of 50 to 90% of the F value. The effect of the web depth is obvious, probably because the flanges become more likely to move laterally as the web depth increases. Where the unbraced length exceeds 1 m, the buckling restraint effect of the sheathing becomes pronounced. The applicability of the proposed equations to channels of large web depth like 235LCN12 is not fully examined and will have to be studied through experiments and other methods in the future.

6. Conclusions

The structural characteristics of panels made by connecting steel channels and plywood with self-drilling screws were investigated experimentally and analytically. Based on the experimental and analytical results, design methods were proposed that appropriately evaluate the composite action and the buckling restraint effect of the plywood. The results obtained allow an economical design of steel-framed houses and improvement of channel strength. The findings of this study may be summarized as follows:

1) The bending tests of the panels quantitatively indicated that the composite action of the channels and plywood and the buckling restraint effect by the plywood were considerable, and clarified the need for design methods considering these effects.
2) It was demonstrated experimentally and analytically that when a panel was subjected to positive bending, the lateral buckling of its channels was fully restrained. It was also indicated that when a panel was subjected to negative bending, the composite action of its channels and plywood was small.
3) A strength evaluation method that takes the composite action of the channels and plywood into account was proposed, and its va-

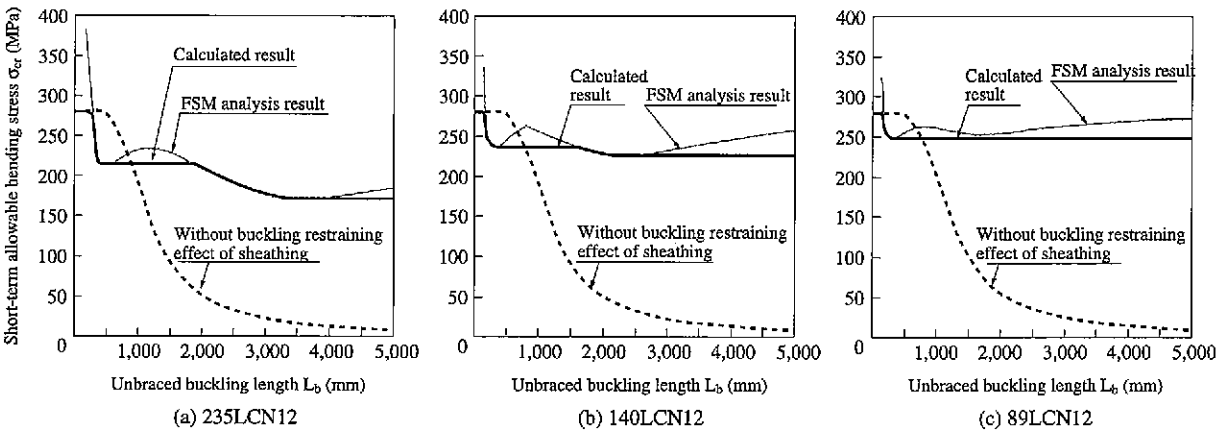

Fig.23 Relationship between short-term allowable bending stress and buckling length of steel-framed house panels subjected to negative bending

lidity was verified. The proposed evaluation method can also evaluate the strength of the panels whose channels and plywood are not fully composite. The evaluation equations were found to be effective when applied to the design of steel-framed houses with standard specifications.

4) When a panel was subjected to negative bending, the plywood in tension was found to restrain the lateral buckling of the channels, resulting in causing a different mode of buckling (distortional buckling) and raising the strength of the panel. A method was proposed for evaluating the buckling strength of the panels based on elastic buckling analysis. Its validity was verified, and its practical effectiveness for steel-framed houses was quantitatively demonstrated.

References

1) Supervised by Bureau of Housings, Ministry of Construction: Design Standard for 2×4 Home, 1992. Japan 2×4 Builders Association, 1992, p. 645 (in Japanese)
2) Kozai Club: Zinc-Coated Light Gauge Steels for Buildings Structure. 1997.7, 21p. (in Japanese)
3) Kozai Club: Self-Drilling Screws for Steel-framed house. 1997.6, 26p. (in Japanese)
4) Kawai, Y., Kanno, R., Hanya, K.: Cyclic Shear Resistance of Light Gauge Framed Walls. Structures Congress '97, 1997, ASCE, p.433-437. (in Japanese)
5) Kozai Club: Design Standard for Steel-Framed House. 1997.5. (in Japanese)
6) Hanya,K., Kanno,R.: Flexural Test of Composite Panels Consisting of Cold-Formed Steel Channels and Plywood with Self-Drilling Screws. Summaries of Technical Papers of Annual Meeting, AIJ, 1996. (in Japanese)
7) Hanya,K., Kanno,R.: Flexural Strength of Composite Panels Consisting of Cold-Formed Steel Channels and Plywood, Part1-3. Summaries of Technical Papers of Annual Meeting, AIJ, 1997. (in Japanese)
8) Hanya, K., Kanno, R., Kawai, Y.: Study on Composite Panels Consisting of Cold-Formed Steel Channels and Plywood with Self-Drilling Screws. Structures Congress '97, 1997, ASCE, p.428-432. (in Japanese)
9) Yu, Wei-Wen: Cold-Formed Steel Design. 2nd ed. John Wiley & Sons, 1991, 631p.
10) Hancock, G.J.: Design of Cold-Formed Steel Structures. 2nd ed. Australian Institute of Steel Construction, 1988, 240p.
11) American Iron and Steel Institute: Specification for the Design of Cold-Formed Steel Structural Members. 1986 Edition with 1989. Addendum, AISI, 1989, 82p.
12) AIJ: Recommendation for the Design and Fabrication of Light Weight Steel Structures. 1985, 215p. (in Japanese)
13) Johnson, R.P.: Composite Structures of Steel and Concrete. Vol. 1. 2nd ed. Blackwell Scientific Publications, 1994, 210p.
14) The University of Sydney, School of Civil and Mining Engineering: THIN-WALL Ver. 1.2 A Computer Program for Cross-Section Analysis and Finite Strip Buckling Analysis of Thin-Walled Structures. 1995, 27p.
15) Papangelis, J.P., Hancock, G.J.: Computer Analysis of Thin-Walled Structural Members. Computers and Structures. 56(1), 157-176 (1995)
16) Kato,B., Akiyama,H.: Elastic Lateral Buckling of H-Beam with a Binded Upper Flange. Journal of Structural and Construction Engineering. (232),41-49(1995)(in Japanese)
17) Kwon, Y.B., Hancock, G.J.: Tests of Cold-Formed Channels with Local and Distortional Buckling, J. of Structural Engineering. 117(7), 1786-1803(1992)
18) Serrette, R.L., Pekoz, T.: Distortional Buckling of Thin-Walled Beams/Panels, I Theory and II Design Methods, J. of Struc. Eng. 757-776 (1995)
19) AIJ: Recommendation for Stability Design of Steel Structures. 1996.1, 367p. (in Japanese)
20) Hanya,K, Kanno,R.: Flexural Strength under Negative Bending of Composite Panels for Steel Framed Houses. Summaries of Technical Papers of Annual Meeting, AIJ, 1998. (in Japanese)